

Narrow-escape-time problem: the imperfect trapping case

Félix Rojo,¹ Horacio S. Wio,² and Carlos E. Budde¹

¹*Fa.M.A.F., Universidad Nacional de Córdoba, Ciudad Universitaria, X5000HUA Córdoba, Argentina*

²*Instituto de Física de Cantabria, Universidad de Cantabria and CSIC, E-39005 Santander, Spain*

We present a master equation approach to the *narrow escape time* (NET) problem, i.e. the time needed for a particle contained in a confining domain with a single narrow opening, to exit the domain for the first time. We introduce a finite transition probability, ν , at the narrow escape window allowing the study of the imperfect trapping case. Ranging from 0 to ∞ , ν allowed the study of both extremes of the trapping process: that of a highly deficient capture, and situations where escape is certain (“perfect trapping” case). We have obtained analytic results for the basic quantity studied in the NET problem, the *mean escape time* (MET), and we have studied its dependence in terms of the transition (desorption) probability over (from) the surface boundary, the confining domain dimensions, and the finite transition probability at the escape window. Particularly we show that the existence of a global minimum in the NET depends on the ‘imperfection’ of the trapping process. In addition to our analytical approach, we have implemented Monte Carlo simulations, finding excellent agreement between the theoretical results and simulations.

PACS numbers: 05.40.Fb

I. INTRODUCTION

The time needed for a particle contained in a confining domain with a single small opening to exit the domain for the first time, usually referred as *narrow escape time* problem (NET), finds a prominent place in many domains and fields. For instance in cellular biology, it is related to the random time needed by a particle released inside a cell to activate a given mechanism on the cell membrane ([1–3]). Generally speaking the NET problem is part of the so called *Intermittent processes*, which are used to explain scenarios ranging from animal search patterns ([4]), through the solutions or melts of synthetic macromolecules ([5, 6]), to the manufacture of self-assembled mono- and multi-layers ([7, 8]). Since the work of Berg and Purcell ([9]), research in the NET problem area has experienced a steady growth over time and motivated a great deal of work ([10–21]).

In [19], we have introduced an analytical Markovian model that showed the impact of geometrical parameters and the interplay between surface and boundary paths in the studied confining domain, of a discrete and rectangular shaped nature, for the perfect trapping case. With “perfect trapping” we refer to the particle’s impossibility of return to the system, i.e. once the particle reaches the narrow opening the escape becomes certain. In that work we presented a phase diagram which showed that some combinations of the geometrical parameter and the transport mechanism were required for the existence of an optimal transport (a global minimum in the NET).

In this work we consider the same confining domain and the transport properties that we dealt with in Ref. [19]. However we eliminate the assumption of perfect escape introducing a finite transition probability at the narrow escape window. It is well known that systems description through the “imperfect trapping case” (once in the trap site capture is not certain) are suitable whenever the surface contains ‘deep traps’, capture and re-emission

from a surface that contains sites with several internal states such as the ‘ladder trapping model’, proteins with active sites deep inside its matrix, etc. ([22–25]). Under this new assumption, we have discovered some very interesting results. Particularly we show that the existence of a global minimum in the NET depends on the existence of an imperfection in the trapping process.

The aim of this work is to study the influence of the ‘imperfection’ in the passage through the escape window on the effective diffusion process, and its effect on the NET problem. For that purpose we calculate the time required by the particle to escape from the system (MET). In order to perform our research we exploit Dyson’s theory ([26]), and the notions of *Absorption Probability Density* (APD) ([23]).

The outline of this paper is as follows. In the following section we introduce some general results regarding imperfect trapping process as well as our model, and provide the basic definitions and concepts. We also describe the proposed analytical approach and present the main results. Section III depicts several assorted illustrations for the MET to the narrow opening for different configurations of the system through a comparison between our analytical framework and Monte Carlo simulations. In Section IV we discuss our conclusions and perspectives. Finally, in the Appendix we present the calculations indicated in Section II.

II. ANALYTICAL APPROACH

A. Some general results regarding imperfect trapping

Let us consider the problem of a walker making a random walk in some finite domain with a trap or sink present in the system. We will follow the walker evolution through the system considering the ‘unrestricted’

conditional probability $P(\vec{s}, t|\vec{s}_0, t = 0)$, that is, the probability that a walker is at \vec{s} at time t given it was at \vec{s}_0 at $t = 0$. By ‘unrestricted’ we identify a situation with no traps/sinks present in the system.

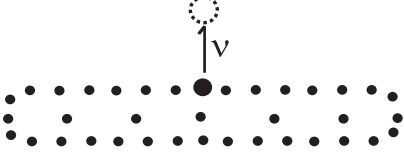


FIG. 1. Finite domain with a trap or sink present. The entrance to the trap site (empty circle) is regulated at the escape ‘window’ by the transition rate ν .

Absorption Probability Density and Mean Absorption Time

As we are interested in the *trapping process*, let us define $A(\vec{s}, t|\vec{s}_0, 0)$ as the *Absorption (trapping) Probability Density (APD)* through the site \vec{s} at time t , given that the walker was at \vec{s}_0 at time $t = 0$, i.e., $A(\vec{s}, t|\vec{s}_0, 0) dt$ gives the trapping probability of the walker, through \vec{s} , between t and $t + dt$ given that it started at $t = 0$ from \vec{s}_0 . It is worth mentioning that the *First Passage time* approach is not fully applicable since an ‘excursion’ to the trapping site does not necessarily ends the process. However we show in the following lines that an interesting relation could be established between $A(\vec{s}, t|\vec{s}_0, 0)$ and $F(\vec{s}, t|\vec{s}_0, 0)$, the *First Passage time density (FPTD)* through the site \vec{s} at time t , given that the walker was at \vec{s}_0 at time $t = 0$.

From now on we will denote the *Laplace* transform of a function $f(t)$ by its argument,

$$\mathcal{L}\{f(t)\} = f(u) = \int_0^\infty e^{-ut} f(t) dt.$$

The connection between the APD and the ‘unrestricted’ conditional probability $P(\vec{s}, t|\vec{s}_0, t = 0)$ could be traced to results in [23] or [27]. This approach in the *Laplace* domain gives,

$$A(\vec{0}, u|\vec{s}_0, t = 0) = \frac{\nu P(\vec{0}, u|\vec{s}_0, t = 0)}{1 + \nu P(\vec{0}, u|\vec{0}, t = 0)}. \quad (1)$$

Let us make a brief digression regarding the relation between the APD and the FPTD. For this we rewrite Eq. (1) in the form

$$A(\vec{0}, u|\vec{s}_0, t = 0) = \frac{P(\vec{0}, u|\vec{s}_0, t = 0)}{P(\vec{0}, u|\vec{0}, t = 0)} \cdot \frac{\nu}{\nu + \frac{1}{P(\vec{0}, u|\vec{0}, t = 0)}} \quad (2)$$

As usual the connection between FPTD and the ‘unrestricted’ conditional probability $P(\vec{s}, t|\vec{s}_0, t = 0)$ is established (in the *Laplace* domain) through the ‘Renewal

approach’ ([28]),

$$F(\vec{0}, u|\vec{s}_0, t = 0) = \frac{P(\vec{0}, u|\vec{s}_0, t = 0)}{P(\vec{0}, u|\vec{0}, t = 0)}. \quad (3)$$

We recognize in equation (2), the FPTD (3) and using the relation $F(\vec{0}, u|\vec{0}, t = 0) = 1 - \Psi(\vec{0}, u)P(\vec{0}, u|\vec{0}, t = 0)^{-1}$, where $\Psi(\vec{s}, \tau)$ is the probability that the walker remains at \vec{s} until time τ since it arrived at \vec{s} at time 0 (in the unrestricted case) [29], we rewrite Eq. (2) as

$$A(\vec{0}, u|\vec{s}_0, t = 0) = F(\vec{0}, u|\vec{s}_0, t = 0) \frac{\nu}{\Psi(\vec{0}, u)^{-1} + \nu} \cdot \frac{1}{1 - \frac{\Psi(\vec{0}, u)^{-1}}{\Psi(\vec{0}, u)^{-1} + \nu} F(\vec{0}, u|\vec{0}, t = 0)} \quad (4)$$

The term $\nu(\Psi(\vec{0}, u)^{-1} + \nu)^{-1}$ in (4) gives the fraction of walkers that are trapped while $\Psi(\vec{0}, u)(\Psi(\vec{0}, u)^{-1} + \nu)^{-1}$ gives the ones that are not absorbed. Further considerations could be made regarding (4), we write it as,

$$A(\vec{0}, u|\vec{s}_0, t = 0) = \sum_{j=1}^{\infty} A_j(\vec{0}, u|\vec{s}_0, t = 0), \quad (5)$$

where

$$A_j(\vec{0}, u|\vec{s}_0, 0) = F(\vec{0}, u|\vec{s}_0, 0) \left(\frac{F(\vec{0}, u|\vec{0}, 0) \Psi(\vec{0}, u)^{-1}}{\Psi(\vec{0}, u)^{-1} + \nu} \right)^{j-1} \cdot \left(\frac{\nu}{\Psi(\vec{0}, u)^{-1} + \nu} \right). \quad (6)$$

Notice that $A_j(\cdot)$ accounts for that walkers that are absorbed in the j -visit ($j = 2, 3, \dots$) and *not before*, i.e., the walkers arrive for the first time at site $\vec{0}$ from \vec{s}_0 but these are not absorbed until they return to site $\vec{0}$ for the $(j - 1)$ -time.

The probability of being absorbed in the j -visit at site $\vec{0}$ is,

$$\int_0^\infty A_j(\vec{0}, t|\vec{s}_0, 0) dt = A_j(\vec{0}, u = 0|\vec{s}_0, 0) = \left(\frac{\Psi(\vec{0}, 0)^{-1}}{\Psi(\vec{0}, 0)^{-1} + \nu} \right)^{j-1} \cdot \left(\frac{\nu}{\Psi(\vec{0}, 0)^{-1} + \nu} \right), \quad (7)$$

where $\Psi(\vec{0}, u = 0)$ is the mean residence time at site $\vec{0}$ in the unrestricted system and we have used that $F(\vec{s}, u = 0|\vec{s}_0, t = 0) = 1$ for a finite (unrestricted) system. As equation (7) shows, when $\nu \rightarrow 0$ independently of the j value, we have no absorption, while in the limit $\nu \rightarrow \infty$ the absorption is certain in the first ‘visit’ to the site (i.e. $j = 1$).

The mean absorption time, i.e., the mean time until the walker is absorbed is evaluated in terms of $A(\cdot)$ as,

$$T = \int_0^\infty t \sum_{\vec{s}_0} A(\vec{0}, t|\vec{s}_0, 0) g(\vec{s}_0) dt = -\frac{\partial}{\partial u} \left\{ \sum_{\vec{s}_0} A(\vec{0}, u|\vec{s}_0, 0) g(\vec{s}_0) \right\} \Big|_{u=0} \quad (8)$$

where $g(\vec{s}_0)$ denotes the probability density of initially finding the walker at a position \vec{s}_0 ([28]).

B. The Model

For our model we consider the problem of a walker making a random walk in a finite rectangular $N \times (M+1)$ lattice (see figure 2). The surface is bounded in the y direction where the walkers can move from $y = 0$ to $y = M$, and periodic boundary conditions are assumed in the x direction so x and $x + N$ denote the same place in space. As we mentioned before, we follow the walker's evolution through the system considering the conditional probability $P(n, m, t | n_0, m_0, t = 0) \equiv P(n, m, t)$, where (n, m) are discrete coordinates in the (x, y) space. $P(n, m, t)$ satisfies the following master equation:

$$\begin{aligned}
 \dot{P}(n, 0, t) &= \gamma P(n, 1, t) - \delta P(n, 0, t) \\
 &\quad + \beta (P(n+1, 0, t) + P(n-1, 0, t)) \\
 &\quad - 2P(n, 0, t); \quad m = 0 \\
 \dot{P}(n, 1, t) &= \delta P(n, 0, t) - 4\gamma P(n, 1, t) \\
 &\quad + \gamma (P(n+1, 1, t) + P(n-1, 1, t)) \\
 &\quad + P(n, 2, t); \quad m = 1 \\
 \dot{P}(n, m, t) &= \gamma (P(n-1, m, t) + P(n+1, m, t)) \\
 &\quad + P(n, m+1, t) + P(n, m-1, t) \\
 &\quad - 4\gamma P(n, m, t); \quad 2 \leq m \leq M-1 \\
 \dot{P}(n, M, t) &= \gamma (P(n-1, M, t) + P(n+1, M, t)) \\
 &\quad + P(n, M-1, t) \\
 &\quad - 3\gamma P(n, M, t); \quad m = M
 \end{aligned} \tag{9}$$

where γ is the surface transition probability per unit time in the x and y direction, β is the transition probability over the line $m = 0$ in the x direction, and δ is the desorption probability per unit time from the boundary line $m = 0$.

We introduce the imperfect escape case by allowing a finite transition probability (ν) at the narrow escape window. Varying from 0 to ∞ , ν allowed the study of both a deficient trapping, and situations where escape is certain (i.e. perfect trapping case).

In the following we will say that the walker ‘escapes’ when it gets trapped or adsorbed, without the possibility of returning to the system. This terminology matches the one used in the NET area. Hence, *adsorption* \rightarrow *escape*, and so on.

Escape Probability Density (EPD)

We now make a brief comment regarding the Escape Probability Density. Taking into account the parameters

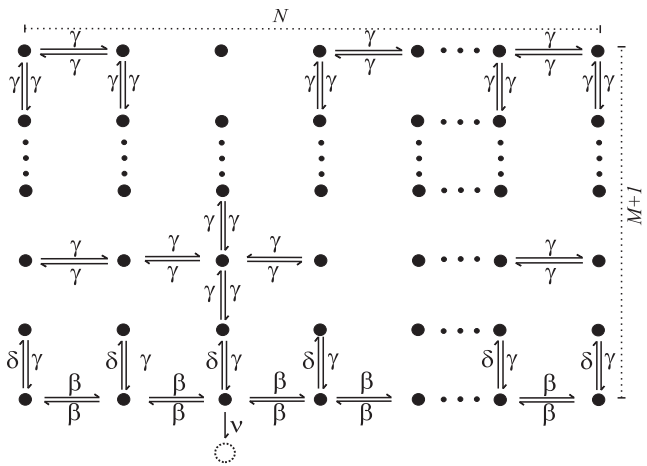


FIG. 2. Schematic transitions of the walker to/from the base line and to/from a generic surface site. Notice that the entrance to the trap/escape site (empty circle) is regulated by the transition rate ν also notice that it could be reached both from the surface (with transition rate γ) and from the baseline (with transition rate β).

of our model, we could write equation (7) as,

$$\begin{aligned}
 \int_0^\infty A_j(\vec{0}, t | \vec{s}_0, 0) dt &= A_j(\vec{0}, u = 0 | \vec{s}_0, 0) \\
 &= \left(\frac{2\beta + \delta}{2\beta + \delta + \nu} \right)^{j-1} \cdot \left(\frac{\nu}{2\beta + \delta + \nu} \right).
 \end{aligned} \tag{10}$$

Notice that as ν grows ($\nu \gg 2\beta + \delta$) each A_j becomes smaller except for A_1 , with $A_1 \rightarrow 1$, i.e. the escape is certain in the first visit. However when $\nu \ll 2\beta + \delta$, the probability of escape $A(\cdot)$ has contributions from each j -visit. This can best be understood considering,

$$\left. \frac{A_j(\cdot)}{A_{j+1}(\cdot)} \right|_{u=0} = 1 + \frac{\nu}{2\beta + \delta} \quad (j \neq 1) \tag{11}$$

which gives the relative contribution of successive terms in (5). When ν gets smaller the contribution is spread all over j values as Eq. (11) shows. In contrast, each $A_j \rightarrow 0$ ($j \neq 1$) as ν grows, concentrating all the probability in A_1 .

Mean Escape Time (MET)

Following the ideas exposed in [19] and by resorting to the matrix formalism and the Dyson's procedure ([26]) we were able to obtain the probability $P(n, m, t | n_0, m_0, t = 0)$ (in the Fourier-Laplace space), which is the building block for the MET. For the detailed calculation see appendix A.

We will denote the (finite) *Fourier* transform by its argument, as we did in the *Laplace* transform case. Thus

for example the transform on a coordinate, say x , would read:

$$P(k, m, t|n_0, m_0, 0) \equiv \mathcal{F} \{P(n, m, t|n_0, m_0, 0)\} \\ = \sum_{n=0}^{N-1} e^{ikn} P(n, m, t|n_0, m_0, 0).$$

From $P(k, m, u|n_0, m_0, t = 0)$ (obtained in the Fourier-Laplace space), the probability that a walker is on the surface at site (n, m) at time t given it was at (n_0, m_0) at $t = 0$, $P(n, m, t|n_0, m_0, t = 0)$, is derived by using the inverse *Laplace* transform on u and the inverse *Fourier* transform on k (for the x coordinate) for each $[\mathbb{P}(k, u)]_{m, m_0}$. However, as we are interested in the calculation of (8), we only need to perform the inverse Fourier transform on $P(0, 0, u|n_0, m_0, t = 0)$, i.e. we need the elements $\mathcal{F}^{-1} \{[\mathbb{P}(k, u)]_{0, m_0}\}$. We obtain for $[\mathbb{P}(k, u)]_{0, m_0}$:

$$[\mathbb{P}(k, u)]_{0, m_0} = \frac{\eta^{m_0} + \eta^{\tilde{M}-m_0}}{\delta(1-\eta)(1-\eta^{\tilde{M}-1}) + (u - A_1(k))(1+\eta^{\tilde{M}})}, \quad (12)$$

where $\eta = 1 + (\tilde{u} - \sqrt{\tilde{u}^2 + 4\gamma\tilde{u}})/2\gamma$, $\tilde{M} = 2M + 1$ and $\tilde{u} = u - A(k)$. The inverse *Fourier* transform on $[\mathbb{P}(k, u)]_{0, m_0}$ is carried out in the following way,

$$P(0, 0, u|n_0, m_0, 0) = \frac{1}{N} \sum_{q=0}^{N-1} e^{i\frac{2\pi n_0 q}{N}} [\mathbb{P}(\frac{2\pi q}{N}, u)]_{0, m_0} \quad (13)$$

Thus we have obtained the required expression for the calculation of the MET through the narrow escape window and it only remains to choose the initial distribution. We now evaluate the MET for a walker with a uniform initial distribution on the base line ($y = 0$). This means the initial distribution is given by $g(n, m) = (1 - \delta_{n,0})\delta_{m,0}/(N-1)$. Notice that we explicitly exclude the possibility of having a walker at $(0, 0)$ at $t = 0$ [30]. This way we obtain,

$$T = N \left[\frac{M}{\gamma} + \frac{1}{\delta} \right] \left\{ \frac{\delta}{\nu} + \frac{\delta}{N-1} \sum_{q=1}^{N-1} \left[\mathbb{P}(\frac{2\pi q}{N}, u = 0) \right]_{0,0} \right\} \quad (14)$$

We make some comments regarding equation (14) which constitutes one of our main results. Notice that (14) adequately provides the limits of perfect escape case, $\nu \rightarrow \infty$ (obtained in [19]) and no escape window, $\nu \rightarrow 0$, $T \rightarrow \infty$. Observe that as it is commented in [16] for a perfect escape case, T could be expressed in the following way,

$$T = \frac{NM}{\gamma} \left[\frac{\delta}{\nu} + \delta \frac{\sum_q [\mathbb{P}(\frac{2\pi q}{N}, u = 0)]_{0,0}}{N-1} \right] \\ + \frac{N}{2\beta} \left[\frac{2\beta}{\nu} + 2\beta \frac{\sum_q [\mathbb{P}(\frac{2\pi q}{N}, u = 0)]_{0,0}}{N-1} \right] \quad (15)$$

or $T = T_{surface} + T_{line}$; (15) provides an interesting physical insight into the problem. Simply notice how the mean

escape time is constructed from the mean duration of *surface* excursions and the mean duration of *border or line* excursions (first and second terms of (15) respectively).

Regarding the existence of a minimum in T

T could be enhanced with respect to δ provided we are able to find $\delta^* = \delta^*(\beta, \gamma, \nu, N, M)$ - the optimal desorption probability - that satisfies,

$$\frac{\partial T}{\partial \delta} \Big|_{\delta=\delta^*} = \frac{NM}{\gamma\nu} + \frac{N}{N-1} \sum_{q=1}^N \frac{M\gamma^{-1}2\beta\alpha_2 - \alpha_1}{(\alpha_1\delta^* + \alpha_22\beta)^2} = 0 \quad (16)$$

where the $\alpha_i = \alpha_i(q, N, M)$ for $i = 1, 2$ are defined in appendix (B). Notice that (16) defines an implicit equation for δ^* which, although we could not solve, provided us with some general conclusions as it approaches certain limits. Consider first $\beta \rightarrow 0$, with the other parameters held fixed. In this case (a finite value for) δ^* exists whenever we have a finite escape probability rate ν and,

$$\delta^* = \sqrt{\frac{\nu\gamma}{M(N-1)} \sum_{q=1}^{N-1} \alpha_1^{-1}}. \quad (17)$$

This is a highly interesting result since in the perfect escape case ($\nu = \infty$) this minimum disappears, as δ^* is pushed towards ∞ . Thus the ‘imperfect’ escape window enables a region that was absent in the perfect case. On the other hand in the limit $\beta \gg \delta$ it could be shown that equation (16) can not be satisfied for any δ^* value. In this case, and taking into account the walker’s initial distribution, the transport is performed on the baseline (lower boundary) of the confining domain, so this is an expected behavior.

In the following section we will make more remarks regarding the minimum in T , while introducing some illustrations corresponding to δ^* .

III. ILLUSTRATIONS

Here we illustrate the general framework introduced in the previous section and compare our theoretical results to independent Monte Carlo simulations. In the next figures, lines indicate analytical calculations while symbols correspond to Monte Carlo (MC) simulations. We will be interested in situations in which a *mixed* type of transport generates a global minimum in the *Mean Escape Time*.

In Fig. 3 we present curves corresponding to the MET (Mean Escape Time), as a function of the desorption rate δ , with parameters $N = 20$, $M = 10$ and $\beta = 0.1$, for different values of the escape ‘strength’ ν , which is the ‘transition rate’ at the escape window. We have included for comparison the ‘perfect escape case’, i.e. once in the escape window the escape is instantaneous, with no

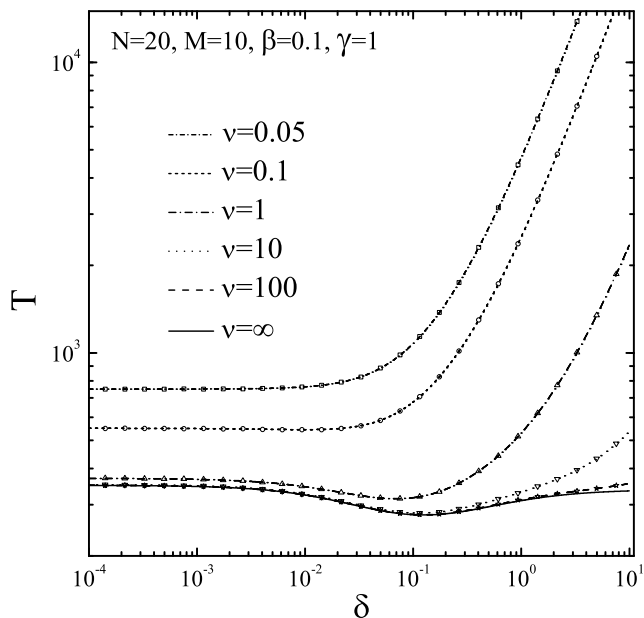


FIG. 3. MET as a function of the desorption rate (in log scale) δ , with $M = 10$, $N = 20$, $\beta = 0.1$, for different values of the transition rate at the escape window ν . From top to bottom $\nu = 0.05, 0.1, 1, 10, 100$. We have also included (thick solid line) for comparison, the *perfect escape window* case ($\nu = \infty$).

dwelling time. Notice how ν regulates the existence of a minimum in the MET: as ν gets smaller the imperfection rises the T curve until it becomes monotonous. Hence, for this situation we could say that ν affects negatively the ‘mixed’ type of transport (journeys along the boundaries and the surface). However it is worth remarking that the transition rate at the escape window can contribute positively as well. This behavior is well depicted in figure 4.

Figure 4 presents curves corresponding to the Mean Escape Time, as a function of the desorption rate δ , with $N = 10$, $M = 2$, $\beta = 0.01$, for different values of the transition rate ν . As can be inferred from the figure, ν significantly influences MET as it varies from 0 to ∞ . Changes in the location of the extrema values of MET can be seen ranging from a monotonous behavior ($\nu \rightarrow \infty$ extrema in $\delta \rightarrow \infty$) to a situation with a global minimum, and then back again into a monotonous behavior ($\nu \rightarrow 0$ extrema in $\delta \rightarrow 0$). So in this case the transition rate to the escape window contributes ‘positively’ to the mixed type of transport, since it turns a situation without a minimum (perfect escape case) into a situation of enhanced transport (minimum in T for some values of ν).

In Fig.5 we present curves corresponding to the δ value that minimizes MET, δ^* , as a function of β for different values of ν , obtained from the numerical solution of Eq. (16). All lines depicts quite a similar trend for finite ν ; $\delta^*(\beta_o, N, M, \gamma, \nu) = 0$ values marked by empty circles are not included in the curves and mark the end of the

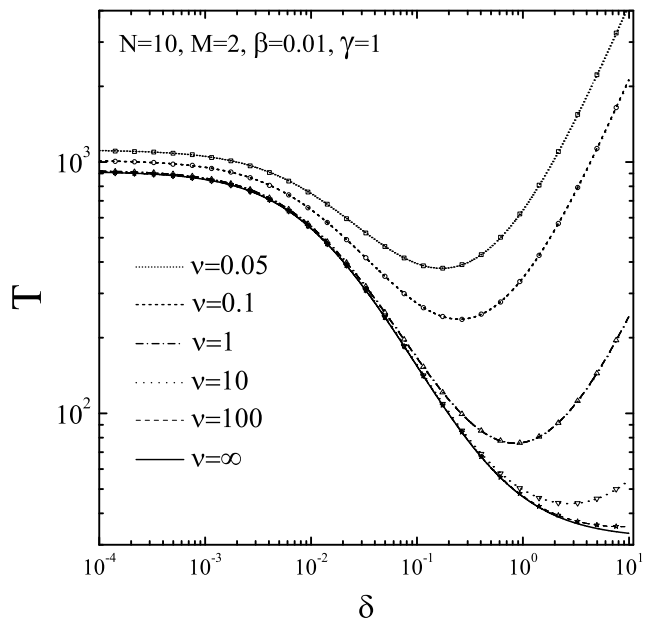


FIG. 4. MET as a function of the desorption rate (in log-log scale) δ , with $\beta = 0.01$, $N = 10$, $M = 2$, for different values of ν (transition rate at the escape window). From bottom to top $\nu = \infty, 100, 10, 1, 0.1, 0.05$. Lines correspond to analytical calculations and symbols to Monte Carlo simulations.

β -interval in which δ^* exists. In other words T is not monotonous while $\beta \in [0, \beta_o)$. As we show in Appendix (B) β_o satisfies,

$$2\beta_o = \frac{\gamma}{M} \frac{\sum_{q=1}^{N-1} \alpha_1 \alpha_2^{-2}}{\frac{(N-1)2\beta_o}{\nu} + \sum_{q=1}^{N-1} \alpha_2^{-1}} \quad (18)$$

For values larger than β_o the T curve reaches a minimum at $\delta = 0$. However this is found at the beginning of the δ -interval and without change of sign of $\partial T / \partial \delta$. We decided to rule it out as long as it doesn’t represent a true interplay between surface and boundary paths. In these situations all particles stay in the base line and eventually escape trough the escape window without excursions into the surface.

The behavior of δ^* considerably changes in the perfect case ($\nu = \infty$). Particularly the range of β values where a minimum exists in T shrinks as indicated by the dashed asymptotes in the figure. The left/right asymptotes indicate the limit in which T becomes monotonous, extrema for $\delta^* \rightarrow \infty$ and $\delta^* \rightarrow 0$ respectively. The left and right asymptotes are respectively located at,

$$2\beta_{\delta^* \rightarrow \infty} = \frac{\gamma}{M} \sum_{q=1}^{N-1} \alpha_1^{-1} \left(\sum_{q=1}^{N-1} \alpha_2 \alpha_1^{-2} \right)^{-1} \quad (19)$$

$$2\beta_{\delta^* \rightarrow 0} = \frac{\gamma}{M} \sum_{q=1}^{N-1} \alpha_1 \alpha_2^{-2} \left(\sum_{q=1}^{N-1} \alpha_2^{-1} \right)^{-1} \quad (20)$$

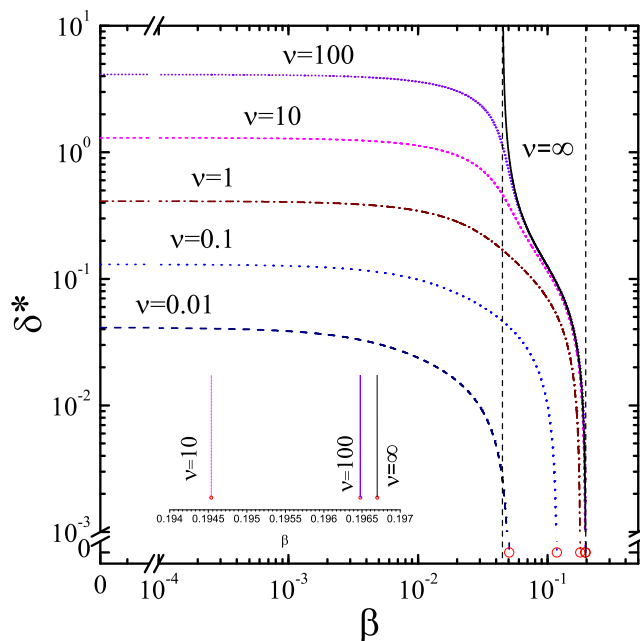


FIG. 5. (color online) δ^* as a function of β (in lin-log;lin-log scale) for fixed N , M and γ for different values of ν . The cuts of δ^* in the β axis ($\delta^*(\beta_o) = 0$) for different ν , indicated by red empty circles are not included in the curve; β_o points are obtained from equation (18). Vertical dashed lines are the asymptotes for the perfect escape case obtained from equations (19) and (20).

For clarity's sake in the inset we have magnified the entry points to the β axis of δ^* curves for $\nu = 10, 100, \infty$.

Figure 6 shows the phase diagrams that summarize the *existence/non-existence* of enhanced transport, analyzed from the perspective of the existence of a minimum in the Mean Escape Time. The diagrams are plotted for fixed N , M and ν as a function of the transition probability over the baseline, β , and the surface transition probability γ . White regions correspond to *non-optimal* transport (absence of minimum -monotonous behaviour- in the MET), while filled regions (red patterns) identify regimes with enhanced transport. We have also included in figure 6, enclosed by black lines the region corresponding to enhanced transport in the perfect window escape case. Dashed curves are obtained from the solution of equation 18 with $\beta_o > 0$,

$$2\beta_o = -\frac{\nu \sum_q \alpha_2^{-1}}{2(N-1)} + \sqrt{\gamma \frac{\nu \sum_q \alpha_2^{-1}}{M(N-1)} + \left(\frac{\nu \sum_q \alpha_1 \alpha_2^{-2}}{2(N-1)} \right)^2}. \quad (21)$$

As it was expected, when ν grows the regions approach the perfect case and the escape, once in the window, becomes certain and instantaneous. Notice that we obtain quite a good agreement between the region of optimal transport, evaluated from equation (14), and the corresponding bounds derived from relations (21) for finite ν

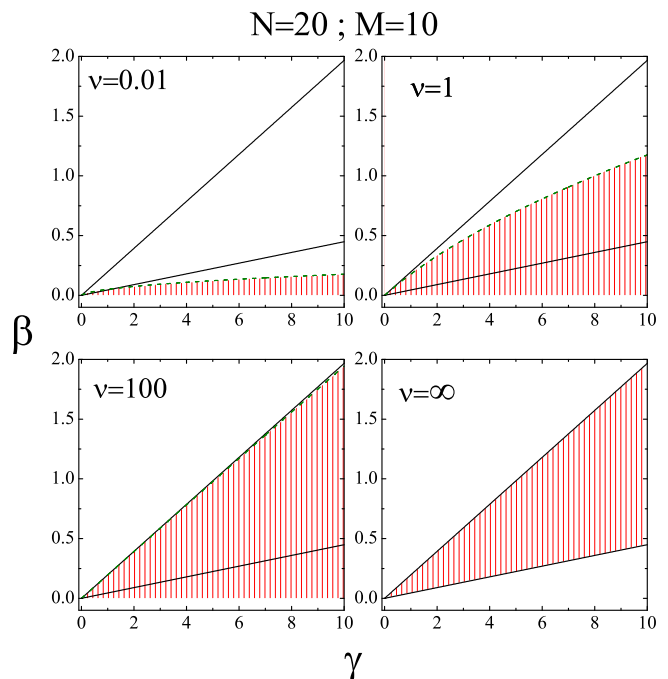


FIG. 6. (color online) Phase diagrams that summarize the *existence/non-existence* of enhanced transport for $\nu = 0.01, 1, 100, \infty$ respectively, for fixed system sizes $N = 20$ and $M = 10$. White regions correspond to *non-optimal* transport, while filled regions (red patterns) identify regimes of enhanced transport. Region enclosed by black lines correspond to enhanced transport in the perfect trapping case ($\nu = \infty$) while dashed (green) lines correspond to the bound -from eq.(18)- after which, T becomes monotonous.

and (19), (20) for $\nu = \infty$.

IV. CONCLUSIONS

We have presented a model based on a master equation approach to the *narrow escape time* problem. In this study we introduced a finite transition probability, ν , at the narrow escape window which allowed us to study the imperfect escape case. Varying from 0 to ∞ , ν allowed the study of both extremes of the trapping process: that of a highly deficient capture, and situations where escape is certain (perfect trapping case).

By resorting to Dyson' technique we have obtained analytic results for the primary quantity studied in the NET problem, the *Mean Escape Time* (MET), and we have studied its dependence in terms of the transition (desorption) probability over (from) the surface boundary, the confining domain dimensions, and the finite transition probability at the escape window. Particularly we showed that the existence of a global minimum in the NET is controlled by the 'imperfection' of the escape process. Regarding such conclusion, a very interesting result was that the 'imperfect' escape window enabled a region

where T could be minimized, something the perfect case lacked.

We have also presented bounds -equations (18), (19) and (20)- between which an optimal minimum value of T could be found, improving previous bounds derived in [19]. The phase diagrams introduced in the last section deserve a special word, for not only do they present a compact summary of the situations of enhanced transport, whenever some exist, but they also can lead to a better understanding of the relations among the parameters that characterize the system. In addition to our analytical approach, we have implemented Monte Carlo simulations, finding excellent agreement between the theoretical results and simulations.

We consider that the presented scheme is an analytically manageable model, which could be used to study the impact of several (domain dimension, different rates of transition, etc.) parameters in the interplay between surface and boundary pathways, and could also serve as a forerunner for the study of more general and complex systems. This work contributes to an area of growing interest, providing a more general overview of a previous work ([19]) and showing a plausible physical insight into the surface-mediated diffusion mechanisms in the presence of an imperfect escape window.

The current approach to the *narrow escape time* problem can be generalized in several directions: higher dimensions, “dynamical” behaviour of the narrow escape window, non-markovian desorption, etc. All of these aspects will be the subject of future work.

ACKNOWLEDGMENTS

The authors thank C. E. Budde Jr. for technical assistance. Support by CONICET and SeCyT (Universidad Nacional de Córdoba), Argentina, is acknowledged. HSW acknowledges financial support from MICINN, Spain, through Project FIS2010-18023.

Appendix A: MET calculation

In this appendix we focus on the calculation of the probability $P(n, m, t | n_0, m_0, t = 0)$, which is the building block for the Mean Escape Time. Taking the (finite) *Fourier* transform with respect to the x variable and the *Laplace* transform with respect to the time t in Equation

(9), we obtain:

$$\begin{aligned}
 & m = 0 \\
 & uP(k, 0, u) - P(k, 0, t = 0) = \gamma P(k, 1, u) \\
 & \quad - (\delta - A_1(k))P(k, 0, u) \\
 & m = 1 \\
 & uP(k, 1, u) - P(k, 1, t = 0) = \delta P(k, 0, u) + \gamma P(k, 2, u) \\
 & \quad - (2\gamma - A(k))P(k, 1, u) \\
 & 2 \leq m \leq M-1 \\
 & uP(k, m, u) - P(k, m, t = 0) = A(k)P(k, m, u) \\
 & \quad + \gamma(P(k, m+1, u) + P(k, m-1, u) \\
 & \quad \quad - 2P(k, m, u)) \\
 & m = M \\
 & uP(k, M, u) - P(k, M, t = 0) = A(k)P(k, M, u) + \\
 & \quad \gamma P(k, M-1, u) - \gamma P(k, M, u).
 \end{aligned} \tag{A1}$$

Here we have defined $A_1(k) = 2\beta(\cos k - 1)$, $A(k) = 2\gamma(\cos k - 1)$. Using the matrix formalism, equation (A1) can be written as

$$[u\mathbb{I} - \mathbb{H}]\mathbb{P} = \mathbb{I}, \tag{A2}$$

where \mathbb{I} is the identity matrix, \mathbb{H} is an $(M+1) \times (M+1)$ tri-diagonal matrix with elements:

$$\mathbb{H} = \begin{bmatrix} C_1 & \gamma & 0 & \dots & \dots & 0 \\ \delta & C & \gamma & 0 & \dots & 0 \\ 0 & \gamma & C & \gamma & 0 & \vdots \\ \dots & 0 & \ddots & \ddots & \ddots & \vdots \\ \dots & \dots & \dots & \gamma & C & \gamma \\ 0 & \dots & & 0 & \gamma & \gamma + C \end{bmatrix}, \tag{A3}$$

C and C_1 are defined as $C = -2\gamma + A(k)$, $C_1 = -\delta + A_1(k)$, and \mathbb{P} is an $(M+1) \times (M+1)$ matrix with components,

$$[\mathbb{P}(k, u)]_{m, m_0} = P(k, m, u | n_0, m_0, t = 0).$$

In order to find the solution to equation (A2) we decompose the \mathbb{H} matrix in the following way,

$$\mathbb{H} = A(k)\mathbb{I} + \mathbb{H}^0 + \mathbb{H}^1 + \mathbb{H}^2, \tag{A4}$$

where

$$\mathbb{H}^0 = \begin{bmatrix} -\gamma & \gamma & 0 & \dots & 0 \\ \gamma & -2\gamma & \gamma & \dots & 0 \\ 0 & \gamma & -2\gamma & \gamma & 0 \\ \dots & \dots & \dots & \dots & \dots \\ \dots & \dots & \gamma & -2\gamma & \gamma \\ \dots & & 0 & \gamma & -\gamma \end{bmatrix}, \tag{A5}$$

corresponds to the transition matrix for a symmetric random walk to nearest neighbours in a finite lattice $(M+1)$

sites) with reflective boundary conditions at the ends. On the other hand:

$$\mathbb{H}^1 = (\gamma - \delta + A_1(k) - A(k))\delta_{i,0}\delta_{0,j} = \Delta_1\delta_{i,0}\delta_{0,j} \quad (\text{A6})$$

$$\mathbb{H}^2 = -(\gamma - \delta)\delta_{i,1}\delta_{0,j} = \Delta_2\delta_{i,1}\delta_{0,j} \quad (\text{A7})$$

$$\begin{aligned} [\mathbb{P}(k, u)]_{m, m_0} &= [\mathbb{P}^0(k, u)]_{m, m_0} + [\mathbb{P}^0(k, u)]_{m, 0} [\mathbb{P}^0(k, u)]_{0, m_0} \cdot \frac{\Delta_1}{1 - \Delta_1 [\mathbb{P}^0(k, u)]_{0, 0}} \\ &+ \frac{[\mathbb{P}^0(k, u)]_{0, m_0} \cdot \Delta_2}{1 - (\Delta_1 + \Delta_2) [\mathbb{P}^0(k, u)]_{0, 0}} \left([\mathbb{P}^0(k, u)]_{m, 1} + \frac{[\mathbb{P}^0(k, u)]_{m, 0} [\mathbb{P}^0(k, u)]_{0, 1} \cdot \Delta_1}{1 - \Delta_1 [\mathbb{P}^0(k, u)]_{0, 0}} \right) \end{aligned} \quad (\text{A9})$$

where,

$$[\mathbb{P}^0(k, u)]_{m, m_0} = \frac{\eta^{|m-m_0|} + \eta^{\tilde{M}-(m+m_0)}}{2\gamma(1-\eta) + \tilde{u}},$$

$$\tilde{u} = u - A(k), \quad \tilde{M} = 2M + 1 \quad \text{and} \quad \eta = 1 + (\tilde{u} - \sqrt{\tilde{u}^2 + 4\gamma\tilde{u}}) / 2\gamma.$$

From (A9), the probability that a walker is at site (n, m) at time t given it was at (n_0, m_0) at $t = 0$, $P(n, m, t | n_0, m_0, t = 0)$ is derived by using the inverse *Laplace* transform on u and the inverse *Fourier* transform on k (for the x coordinate) for each matrix element $[\mathbb{P}(k, u)]_{m, m_0}$. Notice that, as we are interested in the calculation of (8), we only need to perform the inverse Fourier transform on $P(0, 0, u | n_0, m_0, t = 0)$ i.e., we need the elements $\mathcal{F}^{-1} \left\{ [\mathbb{P}(k, u)]_{0, m_0} \right\}$. In this case expression (A9) reduces to,

$$[\mathbb{P}(k, u)]_{0, m_0} = \frac{\eta^{m_0} + \eta^{\tilde{M}-m_0}}{\delta(1-\eta)(1-\eta^{\tilde{M}-1}) + (u - A_1(k))(1 + \eta^{\tilde{M}})} \quad (\text{A10})$$

The inverse *Fourier* transform on $[\mathbb{P}(k, u)]_{0, m_0}$ is carried out in the following way,

$$P(0, 0, u | n_0, m_0, t = 0) = \frac{1}{N} \sum_{q=0}^{N-1} e^{i \frac{2\pi n_0 q}{N}} \left[\mathbb{P}\left(\frac{2\pi q}{N}, u\right) \right]_{0, m_0}. \quad (\text{A11})$$

Thus we have obtained all the required expressions for the calculation of the MET. We now proceed to evaluate the Mean Escape Time for a walker with an uniform initial distribution on the base line ($y = 0$), i.e. $g(n, m) = (1 - \delta_{n,0})\delta_{m,0}/(N-1)$. Notice that we explicitly exclude the possibility of having a walker at $(0, 0)$ at $t = 0$. We obtain,

$$T = N \left[\frac{M}{\gamma} + \frac{1}{\delta} \right] \left\{ \frac{\delta}{\nu} + \frac{\delta}{N-1} \sum_{q=1}^{N-1} \left[\mathbb{P}\left(\frac{2\pi q}{N}, u=0\right) \right]_{0,0} \right\} \quad (\text{A12})$$

A formal solution to equation (A2) is:

$$\mathbb{P} = [u\mathbb{I} - \mathbb{H}]^{-1}. \quad (\text{A8})$$

By applying the Dyson procedure ([26]) a general expression -in the *Fourier-Laplace* space- for $[\mathbb{P}(k, u)]_{m, m_0}$ could be found,

or

$$T = N \left[\frac{M}{\gamma} + \frac{1}{\delta} \right] \left\{ \frac{\delta}{\nu} + \frac{\delta}{N-1} \sum_{q=1}^{N-1} \frac{1}{\alpha_1 \delta + \alpha_2 2\beta} \right\}, \quad (\text{A13})$$

where

$$\alpha_1 = \alpha_1(q, N, M) = \frac{(1 - \eta_{u=0})(1 - \eta_{u=0}^{2M})}{(1 + \eta_{u=0})^{2M+1}} \quad (\text{A14})$$

$$\alpha_2 = \alpha_2(q, N) = 1 - \cos \frac{2\pi}{N} q \quad (\text{A15})$$

Appendix B: δ^* - optimal desorption probability

In this section we present some results regarding the desorption probability rate value that minimizes T, δ^* . For this recall equation (16),

$$\left. \frac{\partial T}{\partial \delta} \right|_{\delta=\delta^*} = \frac{NM}{\gamma\nu} + \frac{N}{N-1} \sum_{q=1}^N \frac{M\gamma^{-1}2\beta\alpha_2 - \alpha_1}{(\alpha_1\delta^* + \alpha_22\beta)^2} = 0 \quad (\text{B1})$$

Let us focus on the relation between δ and β as these are the parameters of interest, since the former enables the transport on the surface, and the later regulates the movement on the boundary line where the escape window is located. Although we will keep track of all variables, it could be shown that (B1) can be written in terms of the scaled variables $\beta' = \beta\gamma^{-1}$, $\nu' = \nu\gamma^{-1}$ and $\delta' = \delta\gamma^{-1}$. So a modification in γ would result in an enlargement or shrinkage (if we let γ get smaller or larger respectively) of the former variables. We will consider the behaviour of $\partial\delta^*/\partial\beta$. Even though we were not able to obtain an explicit expression for δ^* , its derivate with respect to β could be evaluated in closed form. To do this recall equation (B1) and differentiate it with respect to β considering $\delta^* = f(\beta)$ (with the other parameters held fixed).

Then after some algebra we obtain,

$$\frac{\partial \delta^*}{\partial \beta} = \frac{\sum_{q=1}^{N-1} \frac{2(M\gamma^{-1}\delta^*+1)\alpha_1\alpha_2}{(\alpha_1\delta^*+\alpha_22\beta)^3} - \sum_{q=1}^{N-1} \frac{M\gamma^{-1}\alpha_2}{(\alpha_1\delta^*+\alpha_22\beta)^2}}{\sum_{q=1}^{N-1} \frac{(M\gamma^{-1}\delta^*+1)\alpha_1^2}{(\alpha_1\delta^*+\alpha_22\beta)^3} - \sum_{q=1}^{N-1} \frac{M\gamma^{-1}\alpha_1}{(\alpha_1\delta^*+\alpha_22\beta)^2}} \quad (\text{B2})$$

From (B2) we could obtain the entry points to the β axis of δ^* curves. The forerunner for this is the sharp growth on the δ^* curves in figure (5). As a matter of fact the abrupt increase is in $\partial \log \delta^* / \partial \log \beta$. However is not difficult to show that this happens only if the denominator in (B2) $\rightarrow 0$ for some β_o (also notice that in this situation $\delta^* \sim 0$) so,

$$\begin{aligned} \sum_{q=1}^{N-1} \frac{\alpha_1^2}{(\alpha_22\beta_o)^3} &= M\gamma^{-1} \sum_{q=1}^{N-1} \frac{\alpha_1}{(\alpha_22\beta_o)^2} \\ &= (M\gamma^{-1})^2 \left(\frac{(N-1)}{\nu} + 2\beta_o \sum_{q=1}^{N-1} \frac{\alpha_1}{(\alpha_22\beta_o)^2} \right) \end{aligned} \quad (\text{B3})$$

where we have used (B1) to replace the sum on the right hand side. We could go even further and replace the sum on the left hand side. For this we differentiate (B1) with respect to δ^* and get $M\gamma^{-1}2\beta \sum_q \alpha_1\alpha_2(\alpha_1\delta^* + \alpha_22\beta)^{-3} = \sum_q \alpha_1^2(\alpha_1\delta^* + \alpha_22\beta)^{-3}$. By using this relation

and rearranging some terms in (B3) we finally obtain,

$$2\beta_o = \frac{\gamma}{M} \frac{\sum_{q=1}^{N-1} \alpha_1\alpha_2^{-2}}{\frac{(N-1)2\beta_o}{\nu} + \sum_{q=1}^{N-1} \alpha_2^{-1}} \quad (\text{B4})$$

The solution of equation (B4) in terms of β_o that makes $\delta^*(\beta_o, N, M, \gamma, \nu) = 0$ marks the end of the interval in which δ^* exists i.e., the T curve becomes monotonous.

For the perfect escape case we obtain one of the asymptotes between which δ^* exists, outside them the extrema is pushed either to 0 or to ∞ , by letting $\nu \rightarrow \infty$ in (B4),

$$2\beta_{\delta^* \rightarrow 0} = \frac{\gamma}{M} \frac{\sum_{q=1}^{N-1} \alpha_1\alpha_2^{-2}}{\sum_{q=1}^{N-1} \alpha_2^{-1}}, \quad (\text{B5})$$

For the second asymptote we go back to (B2), follow a similar reasoning that lead us to equation (B3), here $\nu = \infty$, $\delta^* \rightarrow \infty$, and obtain,

$$2\beta_{\delta^* \rightarrow \infty} = \frac{\gamma}{M} \frac{\sum_{q=1}^{N-1} \alpha_1^{-1}}{\sum_{q=1}^{N-1} \alpha_2\alpha_1^{-2}}. \quad (\text{B6})$$

Equations (B5) and (B6) constitute an improvement to the bounds derived in [19] and the solution of equation (B4) gives a bound (we could not find similar results in the literature known by us) regarding the existence of a minimum in the MET.

-
- [1] G. Tkačik and W. Bialek, Phys. Rev. E **79**, 051901 (2009).
- [2] M. A. Lomholt, B. van den Broek, S.-M. J. Kalisch, G. J. L. Wuite, and R. Metzler, Proc. Natl. Acad. Sci. **106**, 8204 (2009).
- [3] O. Bénichou, C. Loverdo, and R. Voituriez, EPL **84**, 38003 (2008).
- [4] M. G. E. da Luz, A. Grosberg, E. P. Raposo, and G. M. Viswanathan, J. Phys. A: Math. Theor. **42**, 430301 (2009).
- [5] P. G. de Gennes, Advances in Colloid and Interface Science **27**, 89 (1987).
- [6] J. F. Douglas, H. E. Johnson, and S. Granick, Science **262**, 2010 (1993).
- [7] O. V. Bychuk and B. O'Shaughnessy, Phys. Rev. Lett. **74**, 1795 (1995).
- [8] J. H. Clint, *Surface Aggregation* (Chapman and Hall, New York, 1992).
- [9] H. Berg and E. Purcell, Biophysical **20**, 193 (1977).
- [10] O. G. Berg, R. B. Winter, and P. H. Von Hippel, Biochemistry **20**, 6929 (1981).
- [11] J. Linderman and D. Lauffenburger, Biophysical **50**, 295 (1986).
- [12] H.-X. Zhou and R. Zwanzig, The Journal of Chemical Physics **94**, 6147 (1991).
- [13] I. V. Grigoriev, Y. A. Makhnovskii, A. M. Berezhkovskii, and V. Y. Zitserman, The Journal of Chemical Physics **116**, 9574 (2002).
- [14] A. Singer, Z. Schuss, D. Holcman, and R. Eisenberg, Journal of Statistical Physics **122**, 437 (2006); A. Singer, Z. Schuss, and D. Holcman, *ibid.* **122**, 465 (2006); A. Singer and Z. Schuss, Phys. Rev. E **74**, 020103 (2006).
- [15] P. C. Bressloff and B. A. Earnshaw, Phys. Rev. E **75**, 041915 (2007).
- [16] O. Bénichou and R. Voituriez, Phys. Rev. Lett. **100**, 168105 (2008).
- [17] G. Oshanin, M. Tamm, and O. Vasilyev, The Journal of Chemical Physics **132**, 235101 (2010).
- [18] O. Bénichou, D. Grebenkov, P. Levitz, C. Loverdo, and R. Voituriez, Phys. Rev. Lett. **105**, 150606 (2010); Journal of Statistical Physics **142**, 657 (2011).
- [19] F. Rojo and C. E. Budde, Phys. Rev. E **84**, 021117 (2011).
- [20] R. Walder, N. Nelson, and D. K. Schwartz, Phys. Rev. Lett. **107**, 156102 (2011).
- [21] T. Calandre, O. Bénichou, D. S. Grebenkov, and R. Voituriez, Phys. Rev. E **85**, 051111 (2012).
- [22] J. W. Haus and K. W. Kehr, Physics Reports **150**, 263 (1987).
- [23] M. A. Ré and C. E. Budde, Phys. Rev. E **61**, 1110 (2000).
- [24] W. Nadler and D. L. Stein, The Journal of Chemical Physics **104**, 1918 (1996).
- [25] M. Coppey, O. Bénichou, R. Voituriez, and M. Moreau, Biophysical Journal **87**, 1640 (2004); A. M. Berezhkovskii and A. V. Barzykin,

- The Journal of Chemical Physics **136**, 054115 (2012).
- [26] J. A. Revelli, C. E. Budde, and H. S. Wio, Journal of Physics: Condensed Matter **17**, S4175 (2005).
- [27] J. L. Spouge, A. Szabo, and G. H. Weiss, Phys. Rev. E **54**, 2248 (1996).
- [28] F. Rojo, P. A. Pury, and C. E. Budde, Physica A **389**, 3399 (2010).
- [29] See [22] and references therein.
- [30] This consideration will help us in the comparison with the perfect escape case and avoids the ‘instantaneous’ escaping in the limit $\nu \rightarrow \infty$.